Journal of Applied Sciences

ISSN 1812-5654

Journal of Applied Sciences 11 (9): 1491-1500, 2011
ISSN 1812-5654 / DOI: 10.3923/jas.2011.1491.1500

Two-Phase Flow Behaviour and Pattern in Vertical Pipes

M.A. Zubir and M.Z. Zainon
Department of Mechanical Engineering, Faculty of Engineering,
University of Malaya, 50603 Kuala Lumpur, Malaysia

Abstract: Two parts of research for two-phase flow study were highlighted which is flow behavior study and a void fraction measurement using Constant Electric Current Method (CECM). Both experiments are using a complete set of two-phase flow system that based on industrial scale. In flow pattern study, the investigation was focusing on the experimental work which based on systematic observation and measurements by using a high speed video camera and a few measurement equipments. Three different inner diameter pipes size of 21, 47 and 95 mm were used. The directions of flow were co-current upward flow and the flow velocity range is from 0.1 to 2.0 m sec^{-1}. The effect of L/D and pipe size to the flow clearly describe from the graphs. To measure the void fraction using the Constant Electric Current Method (CECM) experiment, a same system in the flow pattern experiment was used, plus additional constant electric current supply system and data acquisitions system including LabView software. A constant current power source supplied a DC electric power to a few kids of electrodes inside the pipes. One pair of electrode is used for supplying electric power and the others are for detecting the information of hold-up or film thickness. Data acquisition system recorded the voltage output and analyzing using the LabView software. The value of void fraction and the type of flow pattern were predicted using this method. The results were compared to the predictions of void fraction from various void fraction models and correlations.

Key words: Two-phase flow, flow pattern, flow mapping, void fraction, superficial velocity

INTRODUCTION

Two-phase flow study takes place in a wide range of engineering application for example in the industrial plant, boiler and nuclear reactor. Beside that two-phase flow system are also applied in cooling system either in industrial cooling system or electronic equipments. The fundamental information such as flow pattern, void fraction, phase distribution and pressure loss all are important parameters in designing a two-phase flow system. The requirement for this research can contributed in economic designs, optimization of operating conditions and assessment of safety factor leads to the need for quantitative information. The outcome of two-phase flow studies can be contributed in a lot of application especially in industrial plant, medical application and cooling system.

There are quite a few techniques and methods have been developed in order to measure the void fraction in the two-phase flow. The early and most common method to measure the void fraction is by using the resistance probe. This measurement method has been used by Butterworth and Hewitt (1977). A full insulated needle probe except its tip is connected to the tube wall through the fluid. The conductance between the needle probe tip and the wall is very small when the needle probe is in the gas phase while the conductance will be very high when the needle probe is in the liquid phase. Another technique that has been used to measure the void fraction is by using high-intensity x-ray beam developed by Jones and Zuber (1975). In this technique a detector has been use to determined the resultant intensity of the high-intensity x-ray beam that has passes through the flow. The output signal as a function of time is measured from the instantaneous void fraction.

Constant Electric Current Method (CECM) is an improvement method of the conventional conductance method to measure the void fraction or the liquid film thickness. This method has been developed by Fukano (1998) in order to overcome the disadvantages and the flaws of the conventional conductance method. This experiment will study the flow pattern of two-phase air-water flow and feasibility to measure the void fraction using CECM in three different pipes size.

MATERIALS AND METHODS

All the equipment need to be set up for the experiment based on the experiment requirement.

Corresponding Author: M.A. Zubir, Department of Mechanical Engineering, Faculty of Engineering, University of Malaya, 50603 Kuala Lumpur, Malaysia

Experiment rig: The experimental setup consists of three transparent acrylic pipes with different inner diameters (21, 47 and 95 mm) and 3 m length. The purpose of using transparent acrylic pipes is to observe the flow patterns of two-phase flow. The experiment was an adiabatic co current upward two phase flow. The working fluids of in this experiment were water and air. The experiment rig setup was refer to the Sun *et al.* (2004).Water circulated in the flow loop by water pump and air was supplied by the air compressor. Air introduced into the test pipe section at the water-air mixing section, just before the 3 m vertical pipe. As the two-phase mixture flowing through the test pipe, air was separated and released into the atmosphere at the separator. This is to make sure that, only water (one-phase) flows back into the water reservoir. In addition, separator was designing to release the high pressure of the two-phase flow when flowing from a large-area channel (test pipe) into the small-area channel (pipe). This experiment performed at room temperature (27°C) and atmospheric pressure (101.3 kPa).

In this experiment, the air flow rate was measured from 0.83 to 229.04 L min^{-1} controlled by pressure regulator while the water flow rate measured from 2.55 to 106.34 L min^{-1}. The superficial velocities of air and water obtained by divide the volumetric flow rate with the cross-sectional area of the pipe. The range superficial velocities used are shown in Table 1.

Table 1: Range of gas and liquid superficial velocity

Pipe inner diameter (mm)	Superficial liquid velocity (j_l) (m sec^{-1})	Superficial gas velocity (j_g) (m sec^{-1})
21	0.08 -1.00	0.04-2.00
47	0.03-1.00	0.04-2.20
95	0.006-0.500	0.006-0.500

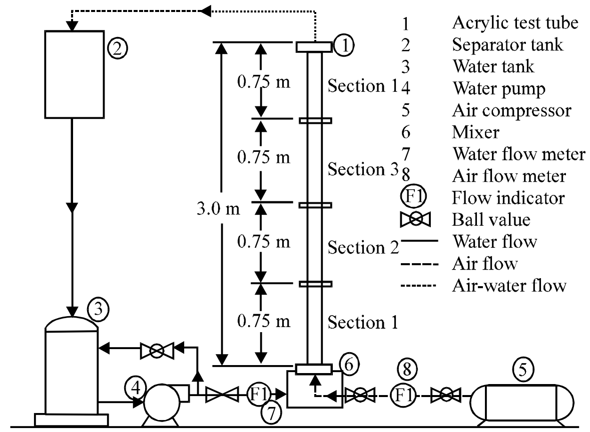

Fig. 1: Schematic view of experiment rig

Flow pattern: There are quite a few techniques have been developed and used to observed the flow patterns such as Neutron Radiography (NR) technique by Mishima *et al.* (1997), X-radiography technique by Heindel *et al.* (2008) and high speed photograph. Generally, the information of the flow pattern is often acquired by visual observation of the flow. The flow patterns inside the tube will manually observed review to the visualization technique by Taylor *et al.* (1963). Another experiment is by Triplett *et al.* (1999) where the flow pattern and the void fraction was measure by a photographs method that taken at the test section. A high-speed photography technique is essential in order to visualize the high velocity flows while for high pressure and high temperature flows needs unique techniques (Triplett *et al.*, 1999). This technique needed a good lighting system with high shuttle speed for a camera and a high frame rate video for video visualization.

In this research, a Digital Single Lens Reflex (DSLR) camera, Casio EX-F1 with a function of high speed video camera was used to capture the flow patterns images throughout the test section (test pipe). A three halogen lamp used to add an extra brightness to the test section during the images capturing process as the amount of light is a vital aspect in the photography method. In the experiment, the 3 m length pipe was divided into four sections and the centre of each section has been identified as the point of observation of the flow patterns. Figure 1 shows the test pipe sections and points of observation. Each section has 0.75 m length and the height from the tube inlet for point 1, 2, 3 and 4 are 0.375, 1.125, 1.875 and 2.625 m, respectively. The flow patterns of the two-phase flow throughout the test section were observed and the images were capture at each section by using the high speed camera. The major disadvantages of using this photography method is that the light is subjected to a complex series of refractions as it passes through the flow and the resultant images of the flow patterns captured are sometimes often difficult to interpret. So the images captured were subsequently processed by proper image processing software in order to refine the images captured and remove any defects.

Void fraction measurement using CECM: Measuring the void fraction in two phase flow system has a few methods. In the industry, a two-phase flow system has a various application in the industrial equipments. Determinations of the characteristic of liquid film in the two phase flow system are important and really useful to have a safe operation, increase performance and save the operational cost for the equipments. In the real industries situation, the two phase flow phenomena cannot be observed through the pipe wall. The flow pattern and the void fraction just can be determined using special

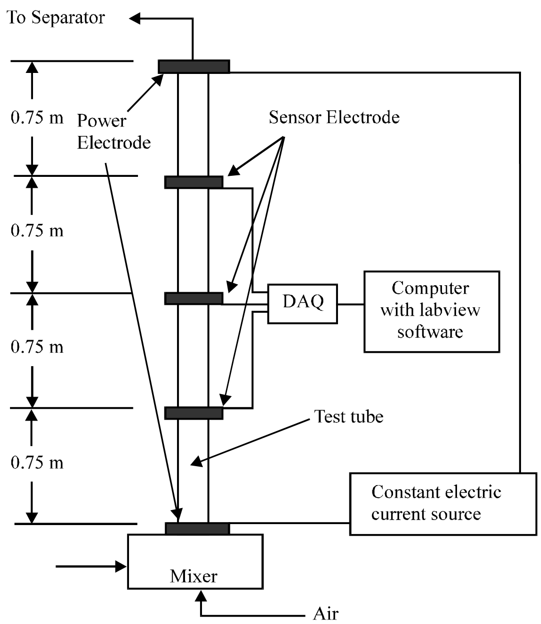

Fig. 2: Schematic view of CECM

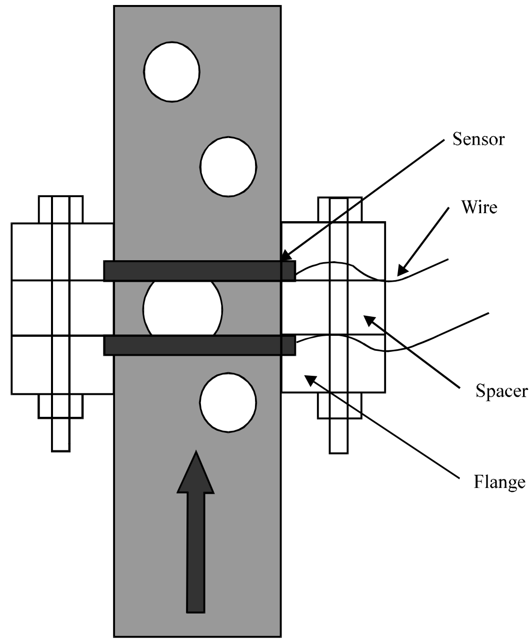

Fig. 3: CECM sensor connection

equipment such x-ray method through the pipe. The x-ray method can cost a lot if running it continuously.

The surface of the liquid film in two phase flow is usually accompanied by various kinds of flow regime complicated wave and that thickness is change with time and position. The interface of the flow conditions in the two phase flow will affect the flow pattern of liquid film, the shear stress on the surface, bubble development condition and the liquid film breakdown in the flow. To accumulate the information of liquid film in real time need a suitable method to and one of the methods is a Constant Electric Current Method (CECM). A simple method like CECM can be apply in the industrial equipment with a low cost budget and can get a real time observation continuously.

In this research, all three test pipes were customized in order to install three pairs of sensor electrodes at three fixed positions which at point 1, 2 and 3 as shown in Fig. 2 with two power electrodes at each of the pipe end. Each pipe is divided into four sections with each section then has 0.75 m length. The sensor electrodes pairs were installed in these flanges while the power electrodes were installed at the inlet and the outlet of the pipe. There were copper wires that connected all the electrodes to a data acquisition (DAQ) module that shown in Fig. 3. The computer with DAQ software was used to observe, analyze and store the experiment data. A static and dynamic calibration was used in this experiment. Different sizes of pipes were put inside the pipe as a referent void for a static calibration. For the dynamic calibration, a liquid flows at constant superficial velocity and different sizes of bubble flows through the pipe as a referent void. The experiment was running in vary liquid and gas superficial velocity while taken the voltage readings. The void fraction value was obtained from the observation by using the formula below:

$$\alpha = \frac{V_L - V_{LG}}{V_L} \qquad (1)$$

Where:

α = Void fraction
V_L = Liquid phase voltage (V)
V_{LG} = Gas-liquid phase voltage (V)

The sampling frequency of the sensor output was at 2 kHz and was processed with a computer. The voltage supply to the pair of electrode was at range of 10 to 30 Volts at 0.3 Amp depend on the pipe size and voltage tapped from sensor.

RESULTS AND DISCUSSION

Flow pattern: Figure 4a-c show the transition of flow patterns in pipe size of 21.0, 47.0 and 95.0 mm ID. From the observation, at fixed liquid superficial velocity, the flow pattern was change with the increase of gas superficial velocity. The bubbly-slug flow appeared in

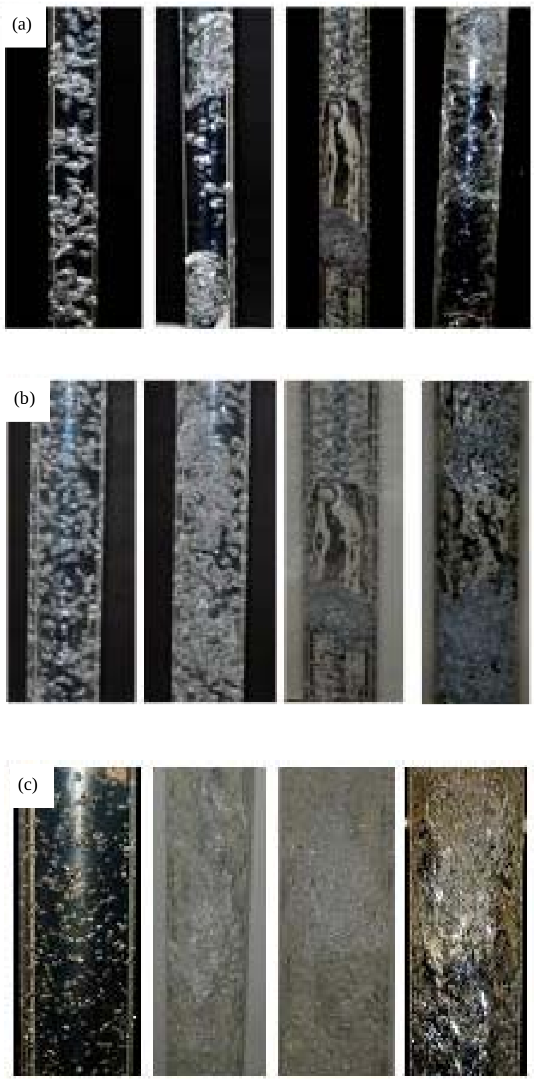

Fig. 4: Flow pattern inside (a) 21mm; (b) 47 mm and (c) 95 mm, ID pipe vertical upward flow

short range in the pipe with low gas superficial velocity. Then the bubbly-slug flow coalesced and formed slug flow afterwards after increase gas superficial velocity.

The slug flow length was different depend on the pipe size. The slug length inside 21 mm ID pipe can approach up to 0.75 m which is the same length of each section of the pipe. For the 47 mm ID pipe, the maximum length of slug was shorter then slug length in 21 mm ID pipe. Inside 95 mm ID pipe, the slug flow was difficult to develop because of the liquid film easy to breakdown to form churn flow. These slug flows were easy to develop at the third and fourth section of the pipe after the coalescing of the bubble in first and second section inside the pipe. The churn flow present at high superficial velocity after the breakdown of liquid film in slug flow. The churn flows were easy to develop inside the 95 mm ID pipe compare with 47 and 21 mm ID pipe.

Flow mapping: In the experiment, each of the 3 m length pipe was divided into four sections and the end of each section has been identified as the point of observation of the flow patterns. Referred to Fig. 1, the test pipe sections and points of observation, each section has 0.75 m length and the height of point 1, 2, 3 and 4 from the pipe inlet were 0.375, 1.125, 1.875 and 2.625 m, respectively.

For the flow pattern observation in 21 mm pipe, the water superficial velocities, J_L range was set from 0.08 -1.0 m sec^{-1} and the air superficial velocities, J_G range is set from 0.04-2 m sec^{-1}, respectively. At low gas superficial velocities and high liquid velocities, the collision frequency of the bubble was very low and the bubbly flow will stay in bubble form if not collided. The bubbles in this pipe are almost uniformly distributed and the shape are small and near spherical. With increase the gas superficial velocity, the patterns were changing to a slug flow when the bubble diameter have as same as pipe diameter.

Figure 5a-d show the flow mapping for 21 mm ID pipe. Analyzing the flow mappings, a different flow pattern distribution respectively with various gas-liquid superficial velocities can be observed. The length of the pipes gives an effect to flow pattern for transit to the other pattern with same gas and liquid superficial velocity. For the 21 mm pipe, the bubbly flow mostly happens at sections 1 and it stays all bubbly at this section till the gas superficial velocity is 0.5 m sec^{-1}. Bubbly flow only happens at all sections at the lowest gas superficial velocity which is 0.04 m sec^{-1} for all liquid superficial velocities. From the observation and tabulated graph, the bubbles inside 21 mm ID pipe were easier to coalesce and form new pattern. Churn flow appeared when the long slug flow liquid film breakdown inside the pipe.

The flow pattern observation in 47 mm pipe shown in Fig. 6a-d, the water superficial velocities, J_L range is set from 0.08-1.0 m sec^{-1} and the air superficial velocities, J_G range was set from 0.04- 2 m sec^{-1}, respectively. The bubbles in this pipe were small in shape and uniformly distributed upward compared to bubble in 21 mm pipe. This flow pattern mostly happens at high liquid superficial velocity and low gas superficial velocities. Referred to the table below, the bubbly flow stays appeared in each section. The collision frequency of the bubble is very low and this pattern will stays as long as the bubble is not large enough and start to collide and coalesce. A slug and

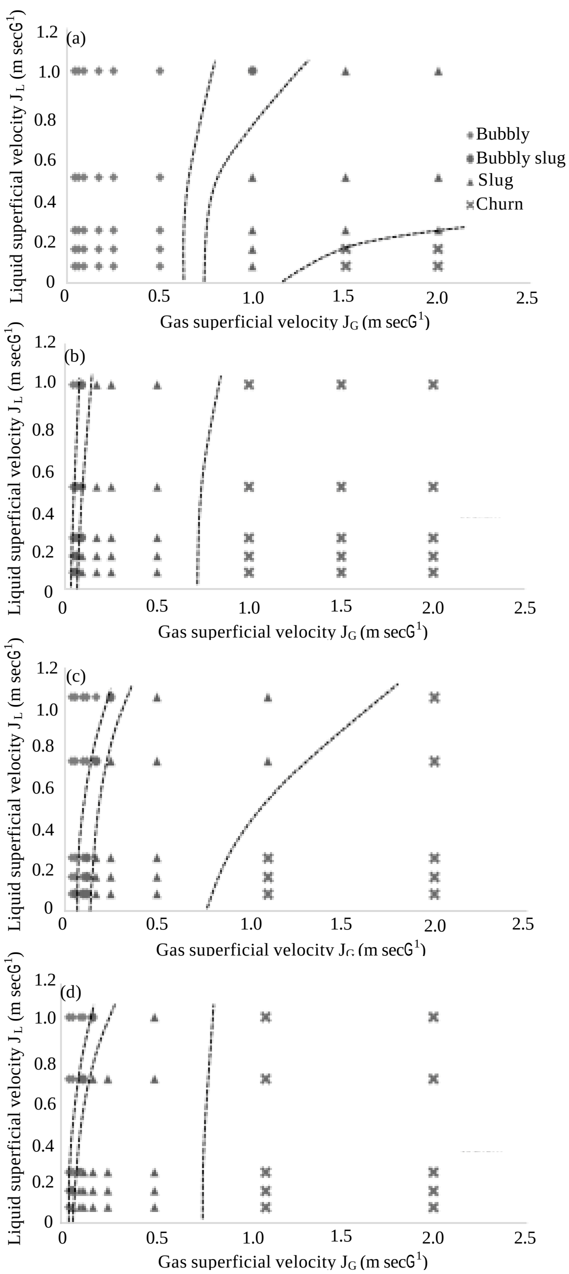

Fig. 5: Flow Pattern Maps for (a) section 1; (b) section 2; (c) section 3 and (d) section 4 in 21 mm ID pipe

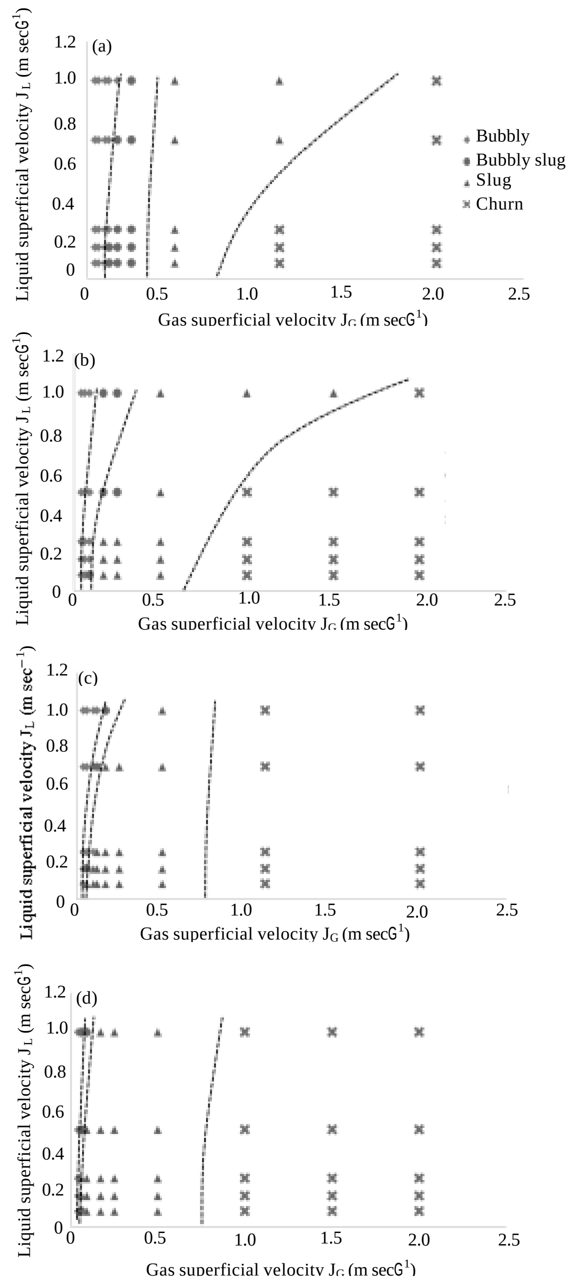

Fig. 6: Flow Pattern Maps for (a) section 1; (b) section 2; (c) section 3 and (d) section 4 in 47 mm ID pipe

churn flow were more difficult to develop inside 47 mm ID compared to 21 mm ID pipes. From Fig. 6, the amount of slug and churn flow are smaller than inside the 21 mm ID pipe. This bubbly-slug pattern is mainly occurs at section 1 and section 2 of this 47 mm pipe when the gas bubbles still not fully collide. This pattern was completely changed in all sections when the gas velocity reached 0.4 m sec^{-1}. As the gas superficial velocity becomes very high the structure of the two-phase flow becomes unstable with the liquid has an oscillatory motion. The churn flow was the last pattern that can be observed in this 47 mm pipe and when the gas superficial velocity achieve above

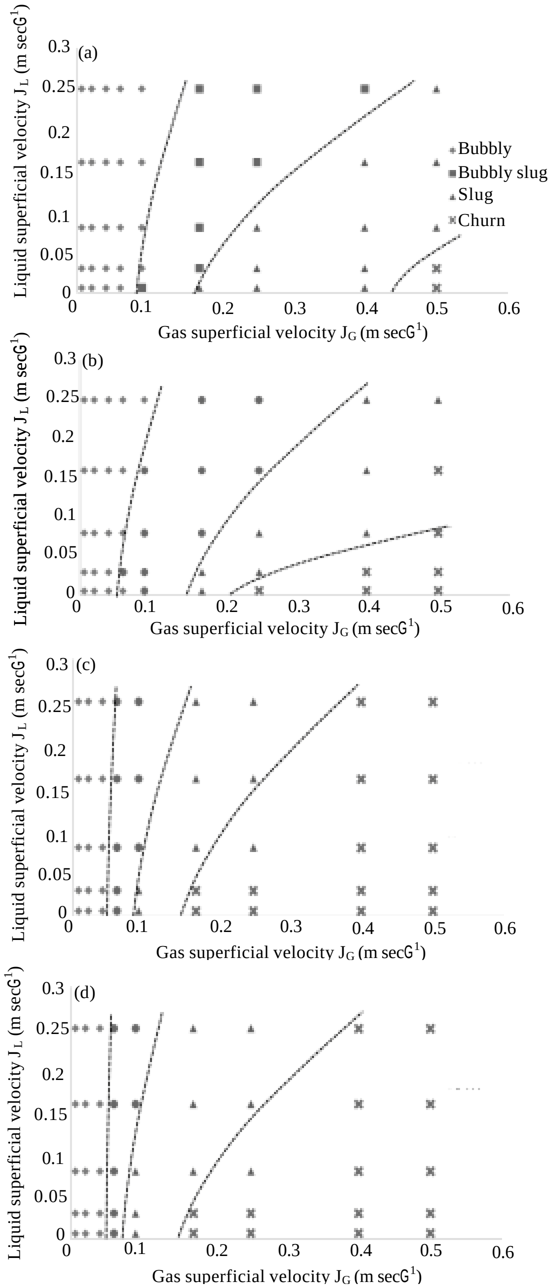

Fig. 7: Flow pattern maps for (a) section 1; (b) section 2; (c) section 3 and (d) section 4 in 95 mm ID pipe

1.1 m sec^{-1}, the churn flow appeared in all section of the pipe. From the observation, the liquid films in slug flow patterns are easily to breakdown to develop churn flow.

As can be seen in this 95 mm pipe at a very low gas superficial velocities range which is 0.006 to 0.04 m sec^{-1}, the bubbly flow pattern was take place at all section for all liquid superficial velocity range. It is only completely

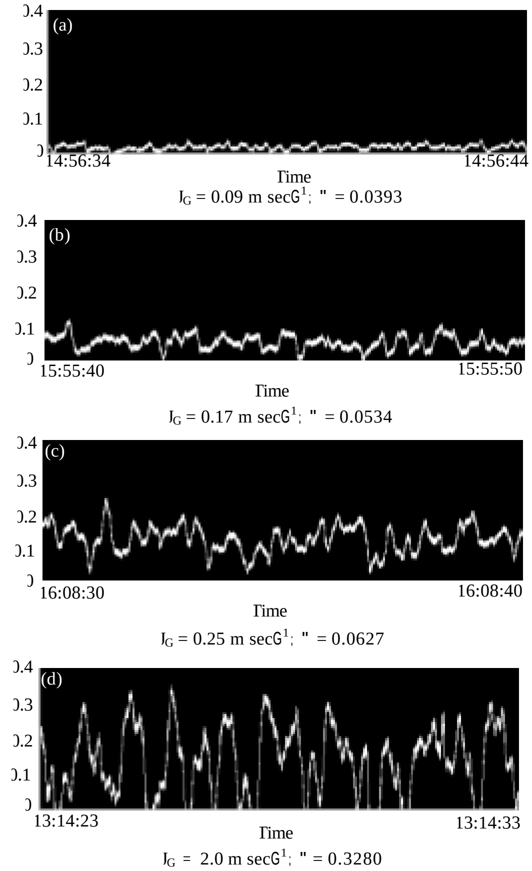

Fig. 8: Void fraction at J_L = 0.25 m/s in 21 mm ID pipe. (a) Bubble flow, (b) Bubbly-slug, (c) Slug flow (d) Churn flow

dissolved at all section for all liquid superficial velocities range when the gas superficial velocity reached 0.17 m sec^{-1} (Fig. 7a-d).

Void fraction: The void fraction was measuring by a developed program using LabView software. The results on average void fraction in each pipe were show in Fig. 8, 9 and 10 which is a time traces of void fraction graph. From the graph can determined the flow pattern type in each pipe with a different gas superficial velocity.

The famous drift flux correlation for the prediction of void fraction is a correlation (Zuber and Finday, 1965) drift flux model (Hibiki and Ishii, 2003). According to the assessment, two of the correlations yielded good predictions over the whole range of void fractions for rod bundle and tube data source.

The absolute error, average error and deviation that are presented in Table 2 are calculated using the following formulas:

$$\varepsilon = \alpha_{meas} - \alpha_{pred} \tag{2}$$

$$\bar{\varepsilon} = \frac{1}{n}\sum_{i=1}^{n}\varepsilon_i \tag{3}$$

$$s = \sqrt{\frac{\sum_{i=1}^{n}(\varepsilon_i - \bar{\varepsilon})^2}{n-1}} \tag{4}$$

The measured of void fractions were compared with predictions by the Bestion drift-flux model. The Bestion drift-flux correlation yields very good results for most of the experiment despite the simplicity of the correlation compared to Chexal-Lellouche drift-flux correlation. The following formula is the Bestion drift-flux correlation:

Table 2: The average error, ε and deviation, s for Bestion and Chexal Lellouche void fraction correlations.

Correlation	Year	Average error (ε)	Deviation (s)
Bestion	1985	0.018	0.088
Chexal-Lellouche	1992	-0.017	0.078

$$C_o = 1v_{gj} = 0.188\sqrt{\frac{gd_h\Delta\rho}{\rho g}} \tag{5}$$

This correlation was chosen based on the good results obtained in a study on the performance of void fraction correlations by Coddington and Macian (2002). The comparison between measured void fraction and Bestion correlation was plotted in graphs that shown in Fig. 11, 12 and 13. The average error and deviation for each pipe was tabulated in Table 3, 4 and 5.

Overall, the average deviation of the measured void fraction from the prediction by Bestion correlation for all pipes was 0.06263 (6.26%). The Bestion correlation predicted well for 95 mm inner diameter pipe with a deviation of 0.02495 (2.5%) followed by the 47 mm inner diameter pipe with 0.07418 (7.42%) and the 21 mm inner diameter pipe with 0.08876 (8.88%). The pipe with 95 mm inner diameter was consistent with the prediction by Bestion correlation with an overall average error of 0.01852. From Fig. 11, it shows that the Bestion correlation

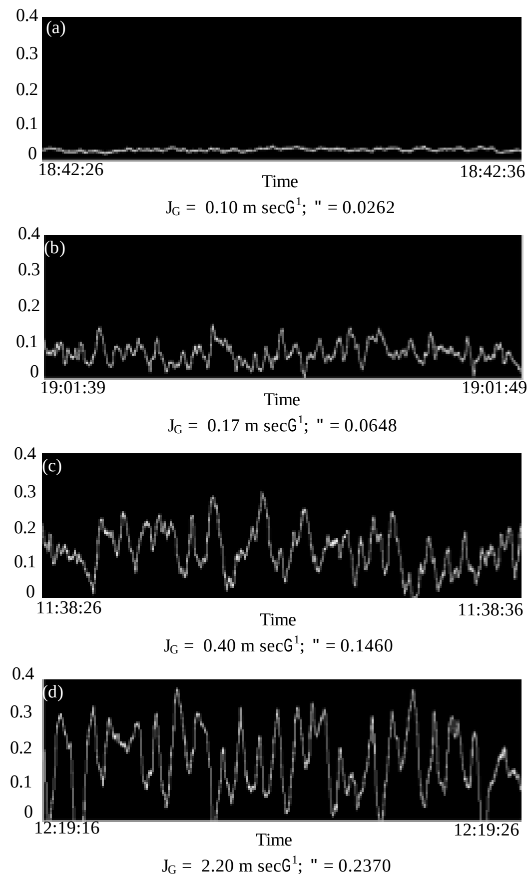

Fig. 9: Void fraction at $J_L = 0.25$ m/s in 47 mm ID pipe. (a) Bubble flow, (b) Bubbly-slug, (c) Slug flow and (d) Churn flow

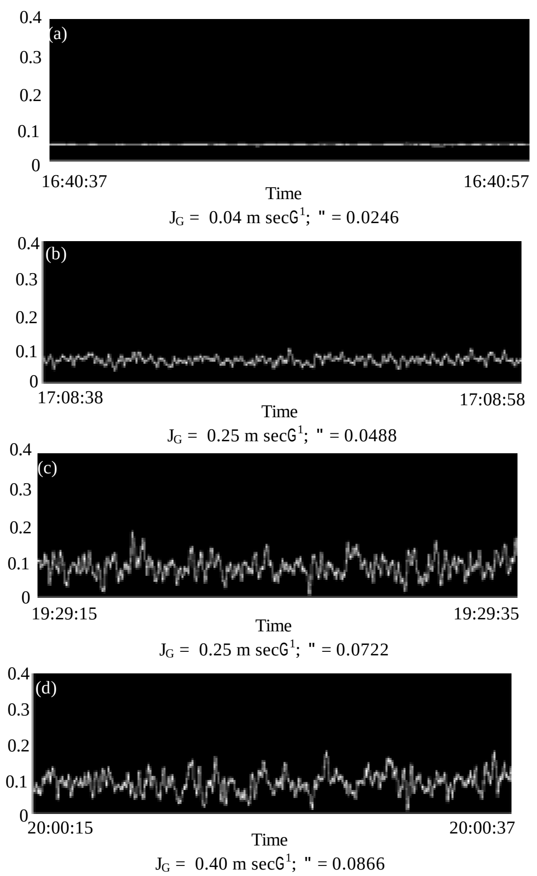

Fig. 10: Void fraction at $J_L = 0.25$ m/s in 95 mm ID pipe. (a) Bubble flow, (b) Bubbly-slug, (c) Slug flow and (d) Churn flow

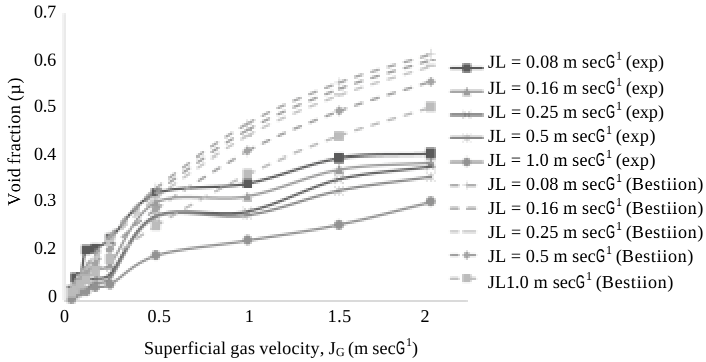

Fig. 11: Comparison measured void fraction and prediction by Bestion correlation for 21 mm ID pipe

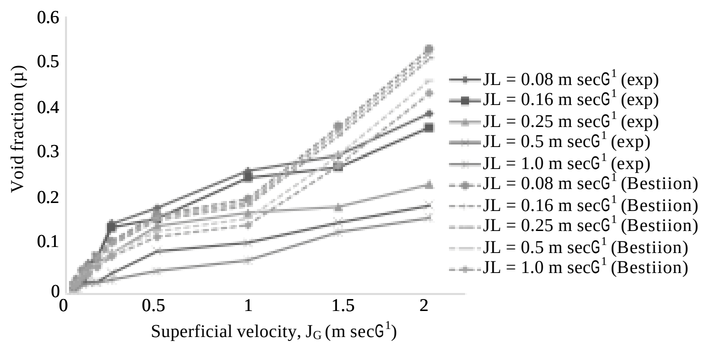

Fig. 12: Comparison measured void fraction and prediction by Bestion correlation for 47 mm ID pipe

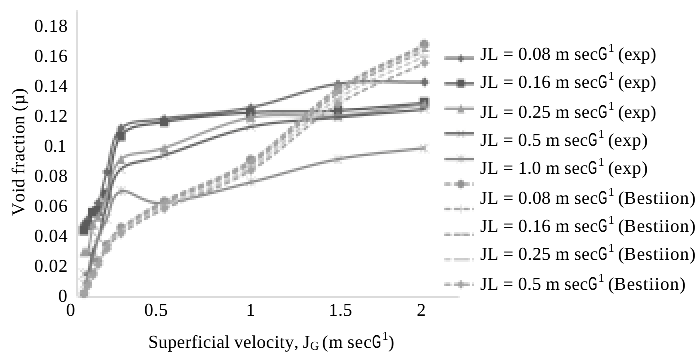

Fig. 13: Comparison measured void fraction and prediction by Bestion correlation for 95 mm ID pipe

Table 3: Average error, ε and deviation, s between the measured void fraction and the prediction by Bestion correlation 21mm ID pipe.

Superficial liquid velocity (J_L)	0.08	0.25	0.50	1.00
Average error (ε)	-0.054	-0.087	-0.081	-0.085
Deviation (s)	0.098	0.088	0.080	0.084

Table 4: Average error, ε and deviation, s between the measured void fraction and the prediction by Bestion correlation 47mm ID pipe.

Superficial liquid velocity (J_L)	0.08	0.25	0.50	1.00
Average error (ε)	-0.010	-0.051	-0.064	-0.069
Deviation (s)	0.0559	0.0895	0.0826	0.0824

under predicts the void fraction before J_L= 0.30 m sec^{-1} and at higher superficial gas velocities, the correlation slightly over predicts the void fraction.

On the other hand, the 21 and 47 mm inner diameter pipes have shown similar trends. The minimum average error in both pipes was found to be at low superficial

Table 5: Average error, ε and deviation, s between the measured void fraction and the prediction by Bestion correlation 95mm ID pipe.

Superficial liquid velocity (J_L)	0.08	0.25	0.50	1.00
Average error (ε)	0.033	0.020	0.013	-0.0007
Deviation (s)	0.025	0.024	0.021	0.025

liquid velocity, J_L. The minimum average error for the 21 and 47 mm inner diameter pipes were -0.0542 and -0.0102, respectively at superficial liquid velocity J_G = 0.08 m sec^{-1}. This shows that the average error increases significantly with the superficial liquid velocity for both pipes. In another case, it was found that the average error increases with superficial gas velocity when the superficial liquid velocity was held constant for both pipes. This error might be caused by the uncertainty of the flow as the two-phase flow transforms from bubble to churn flow.

CONCLUSIONS

From the research, four flow patterns were observed i.e., bubble, bubbly-slug, slug and churn flow. The experimental results indicate that superficial liquid velocity, J_L has a great impact on the flow pattern transition in 21 mm inner diameter pipe. This agrees well with the theory by Butterworth and Hewitt (1977). However, the superficial liquid velocity, J_L did not really affect the flow pattern transition in 47 and 95 mm inner diameter pipe.

Overall, the void fraction increases proportionally to superficial gas velocity, J_G at constant superficial liquid velocity, J_L and decreases with increasing superficial liquid velocity, J_L at constant superficial gas velocity, J_G in all pipes. This really agrees with the experiment done by Triplett *et al.* (1999). In the study of the relationship between void fraction and different pipe diameters, the rise of void fraction with reducing diameter only started at the superficial gas velocity, J_G of 0.5 m sec^{-1} which is during the transition from bubble to slug flow. There was very small difference in the void fraction among the pipes for superficial gas velocity, J_G below 0.5 m sec^{-1}. This agrees well with the theory by Fukano (1998) who has stated that the sensitivity of the CECM is higher in the case of larger void fraction (Fukano, 1998). This theory is most pronounced at J_L = 0.25 m sec^{-1} with the smallest pipe diameter, 21 mm shows a distinctively large void fraction than the other pipes according to size. In addition, the flow pattern can be identified by the characteristic of the void fraction fluctuation with time on waveform charts. This method can be used to monitor flow patterns in pipes in situation of impossible for direct observation.

In the comparison between measured void fraction and Bestion correlation, the Bestion correlation predicted well for the 95 mm inner diameter pipe with 0.02495 (2.5%) deviation followed by the 47 mm inner diameter pipe with 0.07418 (7.42%) and lastly the 21 mm inner diameter pipe with 0.08876 (8.88%). This shows that the Bestion correlation predicts better in larger pipe. Laboratory scale two-phase flow rig and CECM void fraction measurement was successfully constructed based on industrial proportion.

ACKNOWLEDGMENTS

This research was support by University of Malaya research fund and Department of Mechanical Engineering University of Malaya. The author wish to acknowledge the contributions made to this research by research member and undergraduate students.

NOMENCLATURE

C_o	=	Distribution parameter
d_h	=	Hydraulic diameter (m)
g	=	Gravitational acceleration (m sec^{-1})
J_G	=	Superficial gas velocity
J_L	=	Superficial liquid velocity
n	=	Number of data points
s	=	Deviation
v_{gj}	=	Drift velocity (m sec^{-1})
V_L	=	Liquid phase voltage (V)
V_{LG}	=	Gas-liquid phase voltage (V)
α	=	Void fraction
α_{meas}	=	Mean void fraction
α_{pred}	=	Prediction void fraction
ε	=	Average error
ρ	=	Density(kg m^3)
Δρ	=	$\rho_l - \rho_g$ (kg m^3)

REFERENCES

Butterworth, D. and G.F. Hewitt, 1977. Two-Phase Flow and Heat Transfer. Oxford University Press, New York.

Coddington, P. and R. Macian, 2002. A study of the performance of void fraction correlations used in the context of drift-flux two-phase flow models. Nucl. Eng. Des., 215: 199-216.

Fukano, T., 1998. Measurement of time varying thickness of liquid film flowing with high speed gas flow by a Constant Electric Current Method (CECM). Nucl. Eng. Des., 184: 363-377.

Heindel, T.J., J.N. Gray and T.C. Jensen, 2008. An X-ray system for visualizing fluid flows. Flow Measure. Instrum., 19: 67-78.

Hibiki, T. and M. Ishii, 2003. One-dimensional drift-flux model and constitutive equations for relative motion between phases in various two-phase flow regimes. Int. J. Heat Mass Transfer, 46: 4935-4948.

Jones, Jr. O.C. and N. Zuber, 1975. The interrelation between void fraction fluctuations and flow patterns in two-phase flow. Int. J. Multiphase Flow, 2: 273-306.

Mishima, K., T. Hibiki and H. Nishihara, 1997. Visualization and measurement of two-phase flow by using neutron radiography. Nucl. Eng. Des., 175: 25-35.

Sun, X., S. Paranjape, S. Kim, B. Ozar and M. Ishii, 2004. Liquid velocity in upward and downward air-water flows. Ann. Nucl. Energy, 31: 357-373.

Taylor, N.H., G.F. Hewitt and P.M.C. Lacey, 1963. The motion and frequency of large disturbance waves in annular two-phase flow of air-water mixtures. Chem. Eng. Sci., 18: 537-552.

Triplett, K.A., S.M. Ghiaasiaan, S.I. Abdel-Khalik and D.L. Sadowski, 1999. Gas-liquid two-phase flow in microchannels, Part I: Two-phase flow patterns. Int. J. Multiphase Flow, 25: 377-394.

Zuber, N. and J. Findlay, 1965. Average volumetric concentration in two-phase flow systems. J. Heat Transfer, 87: 453-468.